

GC/HRMS Analysis of E-Liquids Complements In Vivo Modeling Methods and can Help to Predict Toxicity

Imari Walker-Franklin,¹ Rob U. Onyenwoke,¹ TinChung Leung, Xiaoyan Huang, Jeffrey G. Shipman, Alex Kovach, and Vijay Sivaraman*



Cite This: *ACS Omega* 2024, 9, 26641–26650



Read Online

ACCESS |

Metrics & More

Article Recommendations

Supporting Information

ABSTRACT: Tobacco smoking is a major risk factor for disease development, with the user inhaling various chemicals known to be toxic. However, many of these chemicals are absent before tobacco is “burned”. Similar, detailed data have only more recently been reported for the e-cigarette with regards to chemicals present before and after the e-liquid is “vaped.” Here, zebrafish were dosed with vaped e-liquids, while C57-BL/6J mice were vaped using nose-cone only administration. Preliminary assessments were made using e-liquids and GC/HRMS to identify chemical signatures that differ between unvaped/vaped and flavored/unflavored samples. Oxidative stress and inflammatory immune cell response assays were then performed using our in vivo models. Chemical signatures differed, e.g., between unvaped/vaped samples and also between unflavored/flavored e-liquids, with known chemical irritants upregulated in vaped and unvaped flavored e-liquids compared with unflavored e-liquids. However, when possible respiratory irritants were evaluated, these agents were predominantly present in only the vaped e-liquid. Both oxidative stress and inflammatory responses were induced by a menthol-flavored but not a tobacco-flavored e-liquid. Thus, chemical signatures differ between unvaped versus vaped e-liquid samples and also between unflavored versus flavored e-liquids. These flavors also likely play a significant role in the variability of e-liquid characteristics, e.g., pro-inflammatory and/or cytotoxic responses.

unvaped vs vaped e-liquids



1. INTRODUCTION

The American Lung Association routinely refers to ~600 ingredients in cigarettes. However, when burned, traditional cigarettes create more than 7000 chemicals, many of which are known to cause cancer and are toxic^a. Similar data have only more recently been reported^{1–5} for the e-cigarette (E-cig) with regards to unused/“unvaped” e-liquid vs those e-liquids that have been heated using an E-cig device to produce an aerosol that is inhaled into the lungs/“vaped”. E-cigs are an emerging form of tobacco products and pose a new danger. The use of E-cig products has increased tremendously, as evidenced by increases in both sales and popularity.^{6,7} In fact, U.S. retail sales for E-cigs have consistently increased and have now surpassed those of combustible cigarettes.^{4,8} For example, total U.S. E-cig sales increased by 46.6%, i.e., from 15.5 to 22.7 million units, during a relatively brief period of time, January 2020–December 2022.⁹ This expanded market has also led to changes within the product itself, resulting in e-cigarettes with varying characteristics.¹⁰ However, although the deleterious effects of cigarette smoking have been documented, significantly less is known about these devices and their potential health effects, which include pulmonary exposures to diverse arrays of chemicals.¹¹

E-cigs differ from conventional cigarettes in that they utilize a battery-operated coil to heat and aerosolize nicotine (if

present) along with a liquid vehicle. The vehicle (e-liquid) is composed of propylene glycol (PG) and vegetable glycerin (VG) at varying ratios and is inhaled directly into the lungs.^{12,13} This new and fast-growing subset of nicotine users, described as “vapers” rather than “smokers”, utilize products that deliver doses of nicotine that achieve plasma nicotine levels comparable to those observed with conventional tobacco smokers.^{14–17} Further, there are 1000 s of varieties of different e-liquid flavors commercially available within a highly dynamic market place. In addition, as data accumulate indicating the adverse effects of E-cig intake, it is becoming clear that a better assessment and regulation of e-liquid is necessary for population safety. For example, small but significant amounts of several carcinogens (e.g., formaldehyde, acetaldehyde, and acrolein) have been detected in E-cig vapors, though these chemicals are absent in the unvaped liquid.^{1,2,18–21} Many of these hazardous chemicals are derived from the flavoring constituents of the e-liquid, such as the case as reported by

Received: April 11, 2024

Revised: May 23, 2024

Accepted: May 27, 2024

Published: June 5, 2024



Allen et al.²² in which the presence of either diacetyl or two other prominent butter-flavored chemicals (2,3-pentanedione and acetoin) was found in 47 of 51 flavored e-liquid aerosols tested. These compounds, traditionally used as the buttery-flavored chemical component in microwave popcorn manufacturing, have been linked to “Popcorn Workers’ Lung”, or bronchiolitis obliterans, which is the scarring of the small airways and can range from mild and reversible to severe and irreversible. Prolonged inhalation of diacetyl results in this disease.^{23,24} A final more recent example pertains to the synthetic cooling agents, e.g., 2-isopropyl-*N*,2,3-trimethylbutyramide (WS-23), and *N*-ethyl-*p*-menthane-3-carboxamide (WS-3), commonly added to e-liquids that impart flavor connotations such as “chilled”, “ice”, “polar”, or “cooled”.^{25,26} Strikingly, a recent study reports that both WS-3 and WS-23 were major components detected in nicotine-containing e-liquids provided by a significant number of e-cigarette, or vaping, product use-associated lung injury patients from August 2019 to June 2021.²⁷ Therefore, it is likely that many more potentially harmful chemicals that possess as of yet unknown, and possibly negative, effects on the lung are also likely to present in flavored e-liquids.

Selections of e-liquid offer a broad range of commercially available flavors, which can be subdivided into the following categories: buttery/creamy, minty, sweet/candy, fruit, tobacco, and cinnamon/spiced,^{28–30} and selecting from these products includes many widely accessible and popular consumer brands of E-cig liquids (e.g., JUUL, Vuse Alto, MyBlu, STIG, and POSH).^{31–33} The study of different e-liquid flavors is highly relevant because there are currently >7000 different flavored e-liquids that are commercially available.¹³ In addition, the number of flavor chemicals composing an e-liquid is highly variable; for example, JUUL uses a relatively small number (<20) of different flavor chemicals in their e-liquid “pods”² while other popular e-liquid refill fluids can contain >50 flavor chemicals.²⁰

While nicotine has been characterized more thoroughly in terms of its physiochemical roles, here we focus upon the less studied flavor chemical constituents of e-liquids. These constituents can be numerous within individual e-liquid products, with 1000 s of e-liquid chemical flavors aerosolized when factoring in the abundance of products available. In particular, our previous studies identified “minty/menthol” flavors, which are flavors previously described as possessing similar flavor chemical characteristics, for example, JUUL “mint” and “menthol” both contain menthol concentrations >10 mg/mL,² as the overall most cytotoxic compound detected.^{33,34} At the same time, our proof-of-concept study also includes our previously developed strategy for the in vivo screening of zebrafish and mice to assess both the safety and mechanism(s) of the toxicity of unvaped vs vaped e-liquids.³⁵ These assays provide us with the ability to prioritize large numbers of flavored e-liquids and to identify their potential toxic components, e.g., particular “minty/menthol” flavor chemicals, using animal models. These models then have the potential to be of great significance, which is illustrated by our investigation of vaped e-liquids, in particular “minty/menthol” flavors, and identify potentially harmful flavor chemicals using oxidative stress and inflammatory immune cell responses as in vivo metrics.

2. MATERIALS AND METHODS

2.1. Materials. Unless otherwise stated, all reagents were purchased from either Thermo Fisher Scientific (Waltham, MA, USA) or Sigma-Aldrich (St. Louis, MO, USA) at the highest level of purity possible. E-cig products, including JUUL pods (“menthol” and “virginia tobacco”, which will be herein referred to as “menthol” and “virginia tobacco”/VT, respectively (both 5% nicotine by weight)), and e-liquids (unflavored, peppermint, spearmint, etc.), were purchased locally from retailers in Durham, NC, USA from May 1, 2022, to April 30, 2023. Products were inventoried and stored at room temperature until used. The manufacturer’s label information for JUUL stated ingredients include only VG, PG, nicotine, flavoring, and benzoic acid. Detailed chemical analyses (gas chromatography–mass spectrometry (GC–MS)) of JUUL pod products have been performed previously² and here as well while utilizing ultrahigh purity helium supplied from Airgas (Pennsylvania, USA) and house nitrogen. Commercial reference standards of nicotine, menthol, and cotinine were purchased from Sigma-Aldrich. Standards of the terpenes (β -caryophyllene, β -pinene, linalool, α -pinene, terpinene, *D*-limonene, and *p*-cymene) were all supplied by the organic synthesis group of RTI International. The first dilution of retention time standards was in methanol (Spectrum Chemical, New Brunswick, NJ, USA), while subsequent dilution was performed in 2-propanol (Fisher Scientific, Hampton, NH, USA). Other analyses were performed here, as described directly below.

2.2. Collecting Vaped E-Liquids. E-liquid was vaped using a previously described^{36,37} apparatus to condensate e-liquid vapor. Briefly, a commercially available device (JUUL, with either (1) the manufacturer’s pods or (2) commercially available and empty, (re)fillable pods filled with e-liquids) was connected to silicon tubing and to the mouthpiece of the device on one end. The other end is placed in the lower part of a 50 mL conical tube in which the e-liquid is condensed and collected, suspended above liquid nitrogen inside a thermal container. Our produced e-liquid vapor condensates and unvaped samples were then utilized for gas chromatography–high-resolution mass spectrometry (GC/HRMS) protocols or for other experiments.

2.3. GC/HRMS. For each unvaped and vaped e-liquid sample, 50 μ L were dissolved in 0.95 mL of isopropanol (IPA) in duplicate and then diluted 1:10 in IPA before being analyzed on a Thermo Scientific (Waltham, MA) Trace 1310 gas chromatograph coupled to a Thermo Scientific Q-Exactive mass spectrometer. One microliter was injected onto a Thermo Scientific LinerGOLD single taper liner with wool (4 \times 6.5 \times 78.5 mm) and separated on a Restek (Bellefonte, PA) Rtx-VMS (30 m \times 0.25 mm ID \times 1.4 μ m film thickness). The inlet temperature was set to 240 $^{\circ}$ C, running 1.2 mL/min of helium as splitless for 0.5 min, followed by a split of 20.0 mL/min (1:33 ratio) for the duration of the run. The initial temperature was set at 45 $^{\circ}$ C and held for 3 min, followed by a ramp at 5 $^{\circ}$ C/min to 100 $^{\circ}$ C, then 2 to 130 $^{\circ}$ C, followed by 5 $^{\circ}$ C/min to 160 $^{\circ}$ C, and finally 20 $^{\circ}$ C/min to 240 $^{\circ}$ C and held for 2 min for a final duration of 41 min. Transfer lines were set at 240 $^{\circ}$ C. The mass spectrometer source temperature was set to 200 $^{\circ}$ C and scanned in full scan positive electron impact (EI⁺) at 70 eV from 40 to 550 *m/z* at 60,000 resolution with a maximum ion trap time of 200 ms and an automatic gain control target of 1×10^6 . A filament delay was set to 6.9 min.

System blanks of IPA were injected prior to sample acquisition of the vaped and unvaped samples, followed by retention time standards. Reference standards were used for confirmation of chemical identities and were determined based on retention time, $[M^+]$ parent ion (calculated using ACD Laboratories ChemSketch Toronto, ON, Canada), and a qualification ion (Thermo Fisher Freestyle software Waltham, MA, USA) using the full scan spectra.

2.4. Nontargeted Analysis Workflow. Thermo Scientific Compound Discoverer (CD) 3.3 software was utilized to complete the nontargeted analysis (NTA) of the samples. The NTA workflow was performed using the GC EI workflow with statistics, which took raw data files from the GC/HRMS deconvoluted the GC EI data, selected relevant spectra, and marked background compounds from predefined blanks selected during sample processing not to be included in the final results. An ion overlap window of 98% was used for the grouping of compounds with no normalization due to no internal standards present for quantitative analysis. Compounds featured included those with a total ion count greater than 100,000, a mass tolerance less than 5 ppm, a peak signal-to-noise ratio greater than 3, and a smoothing of 9. For structural annotation, spectral libraries were used, including the GC-Orbitrap Metabolomics Library (890 spectra), NIST Mainlib (267,376 spectra), and Replib (39,246 spectra), which were all installed with the CD program and utilized high-resolution matches to a library where possible.³⁸ Treatments and sample groups consisted of vaped or unvaped and their unique flavors (peppermint, spearmint, menthol, and unflavored). Volcano plots were utilized to determine significant features when comparing different sample types based on a log fold change in abundance greater than 2 and $p < 0.05$. Principal component analysis (PCA) was used to identify patterns and clusters within the data by determining relationships between feature abundance within the different sample types. Reference standards were used for further identity confirmation of available compounds, and any identities that did not match the retention time standard were excluded.

2.5. High-Throughput Zebrafish Model. The zebrafish platform has proved to be extremely relevant in our previous studies³⁵ and has been used previously to perform inflammation and toxicity assays by other researchers.^{39–42} In this model, the zebrafish AB transgenic strain *Tg(gstp1:GFP)*⁴³ was crossed with the AB wild-type strain. The produced fluorescent embryos were used for the experiment. Zebrafish embryos were washed, dechorionated, and anesthetized before observations. Image acquisition was then carried out through fluorescence imaging for further analysis. All zebrafish experiments were approved by the NCCU IACUC committee.

For chemical treatment and imaging, 1 day postfertilization (dpf) zebrafish embryos were placed in 0.3× Danieau's solution (19.3 mM NaCl, 0.23 mM KCl, 0.13 mM MgSO₄, 0.2 mM Ca(NO₃)₂, 1.7 mM HEPES, and pH 7.0) containing different concentrations (0.05–0.15% [v/v]) of e-liquids, the vehicle control PG/VG or positive control trinitrobenzenesulfonic acid. Fish embryos were maintained at 28.5 °C in 0.3× Danieau's solution containing 30 μg/mL phenylthiourea to inhibit pigmentation. At 2dpf, the embryos were washed, dechorionated, and anesthetized in tricaine before observation. Fluorescence imaging analysis employed an Olympus MVX10 fluorescence microscope (Olympus, Center Valley, PA) equipped with a Hamamatsu C9300-221 high-speed digital

CCD camera (Hamamatsu City, Japan) and VAST BioImager Platform (Union Biometrica, Holliston, MA). MetaMorph Basic software (Olympus) was used for image acquisition and analysis.

For quantification of the oxidative stress response using *nrf2* downstream *gstp1* reporter activity, the fluorescence intensity of the olfactory neural epithelia of *Tg(gstp1:GFP)* fluorescence in zebrafish embryos was quantitated using MetaMorph Basic software. In brief, GFP induction was detectable with fluorescence signal at the area of the olfactory epithelia in the anterior region of the head region. Intensity was measured using an area from a circle with a 60-pixel diameter within the fluorescence olfactory epithelia subtracted from a background nonfluorescent area next to the zebrafish embryo. Both the left and right olfactory epithelia were measured to provide an average fluorescence value. Reported values are averages of measurements from at least 14 embryos.

2.6. Mice and Mouse Exposure Plan. Mice (C57-BL/6J) were purchased from Jackson Laboratories (Bar Harbor, MA, USA). Young adult (6 to 8-week-old male and female) mice were used for all experiments.⁴⁴ After delivery, the mice were allowed to recover from shipping stress for 1 week at the NCCU Animal Resource Complex, which is accredited by the American Association for Accreditation of Laboratory Animal Care. All animal care and use were conducted in accordance with the Guide for the Care and Use of the Laboratory Animals (National Institutes of Health) and approved by the NCCU IACUC. Mice were maintained at 25 °C and 15% relative humidity with alternating 12 h light/dark periods.

To model acute pathology due to vaping, mice received vape exposures using a well-described puff topography of 2 puffs/min (8 s/110 mL/puff, flow rate of 2 L/min)⁴⁵ for 1 h using a M/W/F regime for 5 weeks. This acute exposure model was through nose-cone only administration using an inExpose Nose-Only tower (SCIREQ Inc., Montreal, Canada). This system has been demonstrated to better recapitulate human vaping exposure^{46–48} and can vape up to 12 animals at a time. Body weight and health conditions were monitored daily per the IACUC protocols. Humane endpoints were not used for this study as experimental time points of completion were chosen before any significant body weight change or clinical sign of disease was observed. After the end of the 5-weeks period (within 24 h), mice were humanely euthanized via CO₂ asphyxiation and cervical dislocation, as per our accepted NCCU animal protocol and NCCU Animal Resource Complex housing guidelines and conditions. The sample size was 8 mice (4 male and 4 female) per treatment group.

2.7. Cytokine Analysis. At experimental endpoints, broncho-alveolar lavage (BAL) fluid was collected and frozen as has been previously described.^{49–51} In brief, mice were euthanized, and a catheter attached to a 1 mL syringe was inserted into the trachea. The syringe was then used to deliver 1× PBS, which was gently pipetted up and down 3× to remove the fluid. BAL fluid was then clarified via centrifugation for cytokine analysis. The IL-6 inflammatory cytokine was evaluated by using ELISA (OptEIA, BD Pharmingen) reagents. Experiments were run with an appropriate “*n*” determined by power analysis.

2.8. Histopathology. After being euthanized, the lungs were inflated with 1 mL of a 10% neutral-buffered formalin solution, then removed and suspended in 10% formalin for 12 h. Lungs were washed once in PBS and then immersed in 70% ethanol. Tissues were then embedded in paraffin, and three 5

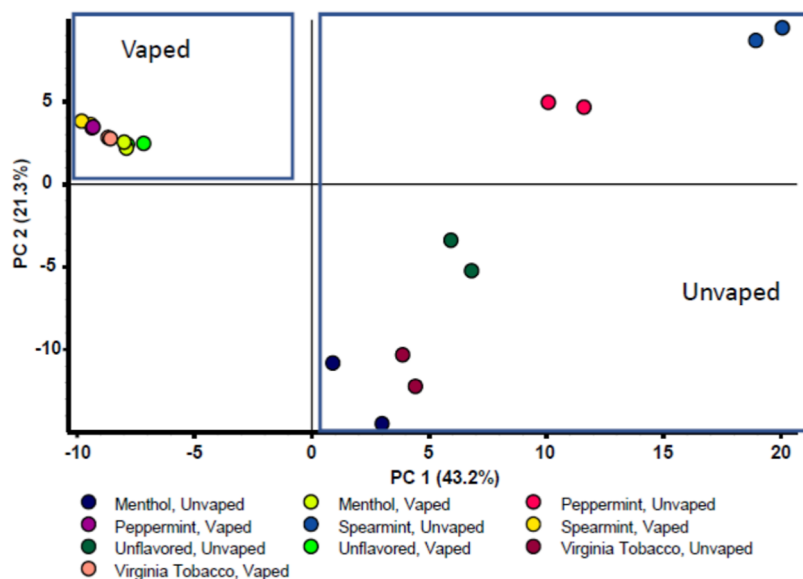


Figure 1. PCA is displaying clustering of vaped vs unvaped samples. The unvaped samples display the unflavored samples in the middle and clustering between the “menthol” and “virginia tobacco” on one side, with peppermint and spearmint samples on the other side.

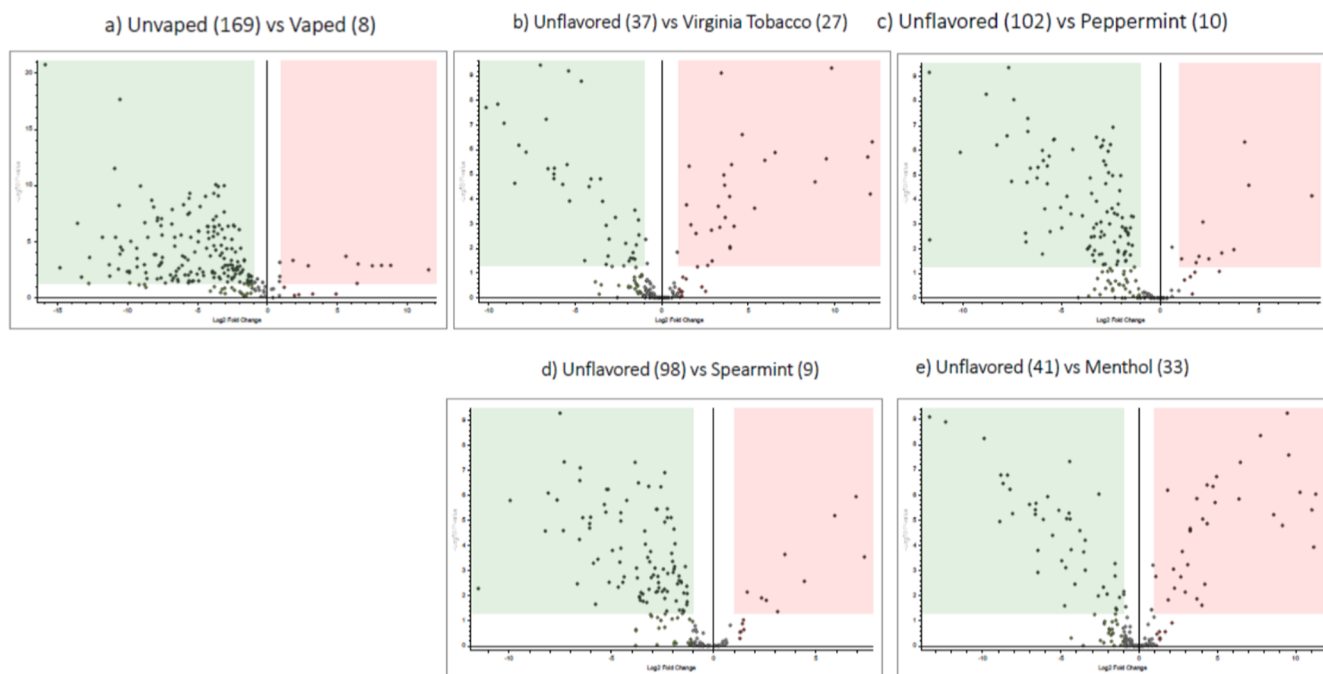


Figure 2. Volcano plots show significant differences between chemical features (log fold change >1 , $p < 0.05$) between sample comparisons of (A) unvaped samples vs vaped samples; (B) unflavored vaped samples vs “VT” flavored vaped samples; (C) unflavored vaped samples vs peppermint flavored vaped samples; (D) unflavored vaped samples vs spearmint flavored vaped samples; and (E) unflavored vaped samples vs “menthol” flavored vaped samples.

μm sections 200 μm apart per lung were stained using hematoxylin/eosin (H&E) for examination by the UNC Cell and Molecular Physiology Histology Core (Chapel Hill, NC). Sections were evaluated blindly for gross pathology.

2.9. Wet/Dry Lung Ratio. Lungs were immediately removed from euthanized mice and weighed (wet weight). The lung tissue was then dried in an incubator (65 °C) for 24 h and reweighed (dry weight). The wet/dry ratio was then calculated by dividing the wet weight by the dry weight.

2.10. Statistical Analysis. Unless otherwise noted, all experiments were performed on a minimum of three separate

occasions ($n = 3$). Data were statistically analyzed using either Student’s t -test or a one-way analysis of variance and compared to the untreated control with Fisher’s Exact Test using GraphPad Prism (La Jolla, CA, USA). Unless otherwise indicated, the results are shown as the mean \pm standard error (SE). A value of $P < 0.05$ is considered as statistically significant.

3. RESULTS

3.1. Comparisons between Vaped Versus Unvaped E-Liquid Samples and Flavored Versus Unflavored E-

Table 1. Selected Features with the Highest NIST Spectral Library Matches and were the Most Significant as Compounds for Vaped Flavored Samples and Organized by the Highest Chromatogram Area^a

Name	CAS	RT [min]	MF	Area Max	Total Score	HRF Score	SI	Sample Type												
								UU	UP	US	UM	UVT	VU	VP	VS	VM	VTV			
Phenylglyoxal	1075-06-5	33.1	C ₉ H ₆ O ₂	9.30E+08	94.1	98.2	739	Blue	Blue	Blue	Blue	Blue	Blue	Blue	Blue	Blue	Blue	Blue	Blue	Blue
L-Menthol ¹	89-78-1	29.1	C ₁₀ H ₂₀ O	8.39E+08	99	99.7	955	Blue	Blue	Blue	Blue	Blue	Blue	Blue	Blue	Blue	Blue	Blue	Blue	Blue
Nicotine ¹	54-11-5	36.5	C ₁₀ H ₁₄ N ₂	1.17E+08	97.8	99.2	908	Blue	Blue	Blue	Blue	Blue	Blue	Blue	Blue	Blue	Blue	Blue	Blue	Blue
Benzoic Acid, TMS	65-85-0*	32.9	C ₁₀ H ₁₄ O ₂ Si	5.31E+07	93.5	98.4	707	Blue	Blue	Blue	Blue	Blue	Blue	Blue	Blue	Blue	Blue	Blue	Blue	Blue
Citronellol	106-22-9	39.5	C ₁₀ H ₂₀ O	3.41E+07	84.3	100	554	Blue	Blue	Blue	Blue	Blue	Blue	Blue	Blue	Blue	Blue	Blue	Blue	Blue
3-Methyl-2-oxovaleric acid, TMS	1460-34-0*	26.7	C ₉ H ₁₆ O ₃ Si	2.73E+07	93.8	100	691	Blue	Blue	Blue	Blue	Blue	Blue	Blue	Blue	Blue	Blue	Blue	Blue	Blue
(-)-Carvone	6485-40-1	33.8	C ₁₀ H ₁₄ O	2.35E+07	98.3	99	934	Blue	Blue	Blue	Blue	Blue	Blue	Blue	Blue	Blue	Blue	Blue	Blue	Blue
Methylvanillin	120-14-9	39.2	C ₉ H ₁₀ O ₃	2.34E+07	99.3	99.6	974	Blue	Blue	Blue	Blue	Blue	Blue	Blue	Blue	Blue	Blue	Blue	Blue	Blue
Tartronic acid, 3TMS	80-69-3*	40.8	C ₁₂ H ₂₀ O ₅ Si ₃	9.15E+06	91.3	91.2	740	Blue	Blue	Blue	Blue	Blue	Blue	Blue	Blue	Blue	Blue	Blue	Blue	Blue
1-Butanal	123-72-8	37.5	C ₄ H ₈ O	8.67E+06	92.3	98.6	643	Blue	Blue	Blue	Blue	Blue	Blue	Blue	Blue	Blue	Blue	Blue	Blue	Blue
(S)-Cotinine ¹	486-56-6	39.3	C ₁₀ H ₁₂ N ₂ O	6.17E+06	98.8	99	961	Blue	Blue	Blue	Blue	Blue	Blue	Blue	Blue	Blue	Blue	Blue	Blue	Blue
Amyl salicylate	2050-08-0	39.2	C ₁₂ H ₁₆ O ₃	4.13E+06	91.8	95.4	680	Blue	Blue	Blue	Blue	Blue	Blue	Blue	Blue	Blue	Blue	Blue	Blue	Blue
Hexanoic acid, TMS	142-62-1*	32.9	C ₉ H ₁₈ O ₂ Si	2.83E+06	82.3	77.6	564	Blue	Blue	Blue	Blue	Blue	Blue	Blue	Blue	Blue	Blue	Blue	Blue	Blue
Caffeine	58-08-2	41.0	C ₈ H ₁₀ N ₄ O ₂	2.21E+06	98.2	99.2	923	Blue	Blue	Blue	Blue	Blue	Blue	Blue	Blue	Blue	Blue	Blue	Blue	Blue
Butyric acid, methyl ester	623-42-7	17.7	C ₈ H ₁₆ O ₂	1.67E+06	85.6	88.5	508	Blue	Blue	Blue	Blue	Blue	Blue	Blue	Blue	Blue	Blue	Blue	Blue	Blue
(-)-Camphor	76-22-2	33.2	C ₁₀ H ₁₆ O	1.58E+06	92.1	99.8	610	Blue	Blue	Blue	Blue	Blue	Blue	Blue	Blue	Blue	Blue	Blue	Blue	Blue
Linalool	78-70-6	19.1	C ₁₀ H ₁₆ O	1.33E+06	92.2	95.1	708	Blue	Blue	Blue	Blue	Blue	Blue	Blue	Blue	Blue	Blue	Blue	Blue	Blue
Terpinene	99-85-4	29.9	C ₁₀ H ₁₆	7.21E+05	91.5	100	572	Blue	Blue	Blue	Blue	Blue	Blue	Blue	Blue	Blue	Blue	Blue	Blue	Blue
Terpineol alpha	562-74-3	29.9	C ₁₀ H ₁₆ O	7.21E+05	88.1	93.9	527	Blue	Blue	Blue	Blue	Blue	Blue	Blue	Blue	Blue	Blue	Blue	Blue	Blue
Salicylaldehyde	90-02-8	7.8	C ₇ H ₆ O ₂	5.94E+05	83.8	82.5	538	Blue	Blue	Blue	Blue	Blue	Blue	Blue	Blue	Blue	Blue	Blue	Blue	Blue
Isomethyl ionone	127-51-5	36.3	C ₁₄ H ₂₂ O	3.79E+05	89.2	87.5	710	Blue	Blue	Blue	Blue	Blue	Blue	Blue	Blue	Blue	Blue	Blue	Blue	Blue
Heptanoic acid, TMS	111-14-8*	7.0	C ₁₀ H ₂₀ O ₂ Si	3.42E+05	92.2	98.7	636	Blue	Blue	Blue	Blue	Blue	Blue	Blue	Blue	Blue	Blue	Blue	Blue	Blue
Linalyl acetate	115-95-7	28.4	C ₁₂ H ₂₀ O ₂	3.04E+05	92.1	99.1	621	Blue	Blue	Blue	Blue	Blue	Blue	Blue	Blue	Blue	Blue	Blue	Blue	Blue
(E)-alpha-Damascene	43052-87-5	37.8	C ₁₀ H ₁₆ O	2.89E+05	91.6	99.4	591	Blue	Blue	Blue	Blue	Blue	Blue	Blue	Blue	Blue	Blue	Blue	Blue	Blue
Benzyl salicylate	118-58-1	12.8	C ₁₄ H ₁₆ O ₃	2.47E+05	74.8	58.2	577	Blue	Blue	Blue	Blue	Blue	Blue	Blue	Blue	Blue	Blue	Blue	Blue	Blue
Damascenone	23696-85-7	37.3	C ₁₀ H ₁₆ O	2.32E+05	87.1	82.2	708	Blue	Blue	Blue	Blue	Blue	Blue	Blue	Blue	Blue	Blue	Blue	Blue	Blue
D-Limonene ¹	5989-27-5	18.1	C ₁₀ H ₁₆	2.07E+05	90.7	87.2	790	Blue	Blue	Blue	Blue	Blue	Blue	Blue	Blue	Blue	Blue	Blue	Blue	Blue
Benzyl Benzoate	120-51-4	39.0	C ₁₄ H ₁₂ O ₂	1.51E+05	93.4	99.1	687	Blue	Blue	Blue	Blue	Blue	Blue	Blue	Blue	Blue	Blue	Blue	Blue	Blue
Bis(2Ethylhexyl)Phthalate	117-81-7	37.2	C ₂₄ H ₃₈ O ₄	1.33E+05	95	100	749	Blue	Blue	Blue	Blue	Blue	Blue	Blue	Blue	Blue	Blue	Blue	Blue	Blue
Lignoceric acid, TMS	557-59-5*	19.9	C ₂₇ H ₅₄ O ₂ Si	8.07E+04	91.1	97.1	612	Blue	Blue	Blue	Blue	Blue	Blue	Blue	Blue	Blue	Blue	Blue	Blue	Blue
Benzyl alcohol, TMS	100-51-6*	32.9	C ₁₂ H ₁₈ O ₂ Si	2.02E+04	83.2	90.3	601	Blue	Blue	Blue	Blue	Blue	Blue	Blue	Blue	Blue	Blue	Blue	Blue	Blue

^aHeatmap included displays the highest (red color) to lowest (blue color) area abundance by a compound. Labeled acronyms: unvaped unflavored (UU), unvaped peppermint (UP), unvaped spearmint (US), unvaped “menthol” (UM), unvaped “virginia tobacco” (UVT), vaped unflavored (VU), vaped peppermint (VP), vaped spearmint (VS), vaped “menthol” (VM), and vaped “virginia tobacco” (VVT). *Cas # is for the parent structure and doesn't include the TMS derivatives. ¹Confirmed compound using reference standards RT time, parent ion [M⁺], and qualifier ion in full scan spectra.

Liquid Samples. To begin to explore differences/similarities between e-liquid samples, a PCA was performed using our obtained GC/HRMS data from vaped versus unvaped samples. Again, our choice of products and study rationale was informed based upon our previous studies^{33,34} using “minty/menthol” flavors combined with the relative popularity of these flavor profiles among commercially available e-liquid products.⁹ When further analyzing these samples, these respective e-liquid samples tend to clearly cluster together, visually displaying both the stark differences between the groups and the high degree of similarity among the sample group members (Figure 1). However, clustering for the unvaped samples was more spread out, with the unflavored samples in the middle. “Menthol” and “VT” samples clustered to the left of the unflavored unvaped, while the spearmint and peppermint clustered to the right side of the unflavored unvaped samples. Similarly, total detected chemical signatures that were significantly upregulated (\log_2 fold change = 1, $p < 0.05$) differ among the unvaped vs the vaped samples with 169 and 8, respectively, unique chemical signatures found to be significantly different (Figure 2A). When assessing differences between a vaped flavored e-liquid versus unflavored e-liquid (Figure 2B–E), similar patterns emerge; i.e., significant differences in flavor compositions exist between a flavored e-liquid, e.g., “menthol”,³³ and the unflavored e-liquid.⁴¹

3.2. Structural Annotation of Features within the Samples. An NTA workflow on the GC/HRMS data was then utilized, resulting in the detection of 228 features within the samples. Structural annotations of 31 selected significant features within the NIST spectral library match >70 high-resolution filtering scores and 500 search indexes (SI) thresholds are displayed in Table 1. Chemical reference standards were used to confirm the identities of 4 compounds (L-menthol, nicotine, cotinine, and limonene). By utilizing the reference standard, an additional menthol isomer was detected within the spearmint-vaped and unvaped samples. Nicotine and its derivative cotinine were found to be upregulated in the unvaped samples, with the highest area of abundance in the VT sample. When surveying these data, some flavorants were more prominent in specific sample types (L-menthol in “menthol” samples and methyl vanillin in VT samples). Terpinene compounds (D-limonene, terpinene, (–)-carvone, (–)-camphor, damascenone, etc.) were annotated throughout the flavored samples. Compounds most significant to vaped samples included citronellol, 1-butanol, amyl salicylate, butyric acid methyl ester, linalool, terpineol α , and isomethyl ionone, with many of these compounds being characterized as potential respiratory irritants.^{52,53} Additional compounds highest in the vaped samples contain trimethyl silica compounds adducted to them, i.e., benzoic acid, 3-methyl-2-oxovaleric acid, tartronic acid, hexanoic acid, heptanoic acid,

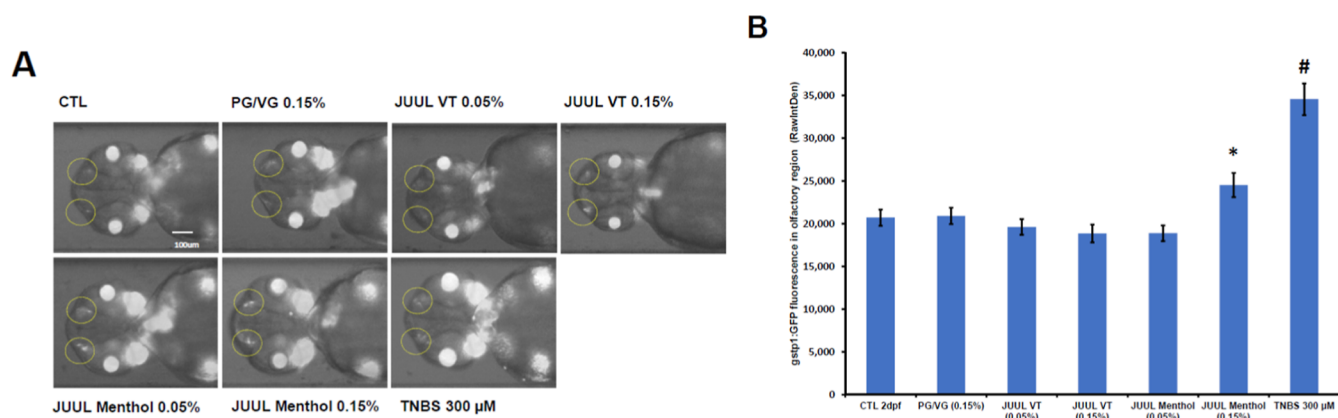


Figure 3. A menthol-flavored e-liquid induced oxidative stress in *Tg(gstp1:GFP)* zebrafish. (A) Oxidative stress-induced Nrf2 responses were measured using *Tg(gstp1:GFP)* fluorescence signal at the olfactory sensory neural epithelia of zebrafish embryos at 2 day-postfertilization (dpf) after a 24 h treatment with the e-liquids dissolved in embryo medium (0.3× Danieau’s solution). Bright field and fluorescence composite images of the ventral view of the head region of *Tg(gstp1:GFP)* zebrafish embryos at 2 dpf. The inducible *gstp1:GFP* activity at the olfactory sensory neural epithelia is indicated by the two dotted circles. CTL is the medium alone. (B) $n = 14–16$ zebrafish embryos per treatment group. * $p < 0.05$, # $p < 0.0001$ using Student’s *t*-test. This study was powered to provide for a more than 95% confidence interval when using Fisher’s exact test.

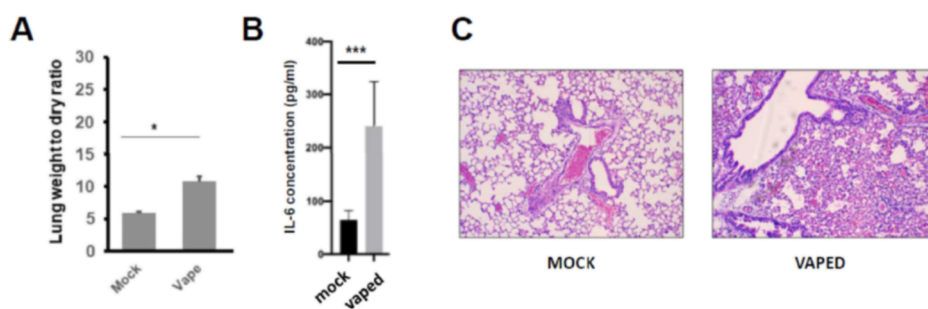


Figure 4. Acute in vivo model of vaping indicates cytotoxicity (A) and lung inflammation (B,C). To model acute pathology due to vaping, mice received vape exposures (“menthol”) using a well-described puff topography of 2 puffs/min (8 s/110 mL/puff, flow rate of 2 L/min) for 1 h each day using an M/W/F regime for 5 weeks. (A) Lung wet/dry weight ratios of mice either unvaped/mock control or vaped. $n = 8$ mice (four male and four female) per treatment group. (B) IL-6 ELISA analysis was run using clarified BAL fluid. $n = 8$ mice (four male and four female) per treatment group (C) H&E staining (100× magnification) of sections of lung tissue isolated from unvaped/mock or vaped mice. Alveolar wall thickening was most observable in the lungs from the vaped mice compared to the mock/unvaped control. $n = 8$ mice (four male and four female) per treatment group. * $p < 0.05$, *** $p < 0.001$ using Student’s *t*-test. This study was powered to provide for a more than 95% confidence interval when using Fisher’s exact test.

lignoceric acid, and benzyl alcohol. TMS-derived library searches also appeared within the Compound Discoverer workflow. It is hypothesized that this is due to the similarity of spectra to the library match without the TMS additive; however, since no derivatization occurred during the GC/HRMS protocols, these are potential false-positives. A similar response happened with multiple peaks at different retention times appearing, where the top library search was used for multiple features—different identities were not applied in the case the compound could be related, such as the case for isomers (D vs L menthol).

3.3. Zebrafish Model Indicates E-Liquid Treatment Induces Oxidative Stress. While not an obvious in vivo model to study the effects of vaping, the zebrafish model has provided a strong platform for our previous studies³⁵ and has been used to perform inflammation and toxicity assays.^{39,40,54} In fact, while using zebrafish embryos, we have previously demonstrated developmental effects and pro-inflammatory response, as indicated by a neutrophil migration response, after treatments with many of the same vaped flavored e-liquids utilized above (VT, “mint”, and “menthol”), with the VT, “mint” and “menthol” e-liquids all inducing pro-

inflammatory responses.³⁵ However, higher concentrations (e.g., 0.0375% “mint”) of e-liquid in the zebrafish medium reduced the survival of the exposed embryos with doses higher than 0.075, 0.05, and 0.025% for “menthol”, “VT” and “mint”, respectively, demonstrated as lethal for zebrafish embryo survival (Onyenwoke et al. 2022).³⁵ However, these earlier studies did inform us of appropriate e-liquid concentrations (0.05 and 0.15%) for further assays, as described below.

Here, we moved to employ an oxidative stress reporter assay (Keap1–Nrf2 interaction^{55,56}) in the zebrafish.⁵⁷ With this assay, oxidative stress-induced Nrf2 responses are measured using *Tg(gstp1:GFP)* fluorescence signal at the olfactory sensory neural epithelia of zebrafish embryos at 2 day-postfertilization (dpf) after a 24 h treatment with the e-liquids dissolved in embryo medium (0.3× Danieau’s solution). Bright field and fluorescence composite images of the ventral view of the head region of *Tg(gstp1:GFP)* zebrafish embryos at 2 dpf are taken. The inducible *gstp1:GFP* activity at the olfactory sensory neural epithelia is then indicated by the two dotted circles. With this assay, we now provide data illustrating that a menthol-, but not a tobacco-flavored, e-liquid induces an acute oxidative stress response in zebrafish embryos (Figure 3).

These new data again illustrate the importance of identifying the individual flavor constituents/chemical signatures between and among various different commercially available e-liquids, harkening back to our GC/HRMS data, and that a “menthol/minty” chemical flavor profile is imparting a likely detrimental toxicity characteristic.

3.4. Secondary In Vivo Model to Assess the Inflammatory Toxicity of Selected Vaped E-Liquids.

The zebrafish neutrophil inflammation *Tg(lysC:dsRed)*³⁵ and oxidative stress response *Tg(gstp1:GFP)* assays are powerful tools for the evaluation of the inflammatory/toxic nature of vaped e-liquids, though a secondary validation step (mouse model) is necessary to more thoroughly interrogate the inflammatory potential of acute and chronic vaping exposure upon mammalian pulmonary function. For this confirmation, we employed an inExpose Nose-Only tower to vape (the “menthol” e-liquid) using a biologically relevant exposure strategy. Upon endpoint of the experiment, we utilized lung weight (wet/dry ratios; Figure 4A) and IL-6 measurements,³⁷ key hallmarks of acute lung injury (ALI)/acute respiratory distress syndrome (ARDS)^{58,59} and of a pro-inflammatory response,^{60,61} respectively, as key measurements. Both metrics displayed an increase, however, only with regard to the vaped animals. These results were corroborated with histopathological assessment of lungs by H&E staining (Figure 4C), confirming the results from zebrafish experiments. Thus, our in vivo data indicate overall cytotoxicity (Figure 4A) and signs of ALI/ARDS and of a pro-inflammatory lung response (Figure 4B,C;³⁷) after vaping alone with a flavored e-liquid, which is in agreement with other e-liquid and e-liquid aerosol studies.^{2,13,60,62–64}

4. DISCUSSION

Preliminary tests with commercially available e-liquids have been successfully performed here to assess the feasibility. For each e-liquid, liquid samples were (1) collected unvaped, and (2) vapor phases were collected and condensed after vaping.^{65–67} Samples were then assessed by GC/HRMS analysis. As initially hypothesized, chemical signatures identified greatly differed between unvaped vs vaped samples (Figures 1 and 2) as well as unflavored versus flavored e-liquids, with known chemical irritants such as, e.g., methyl esters of caproic acid and *cis*-11,14-eicosadienoic acid, and tolualdehyde, present in vaped and unvaped flavored (but not unflavored) e-liquids (Tables S1 and S2).^{68,69} However, possible respiratory irritants, such as terpinene, butyric acid, and methyl ester, were present in vaped e-liquid and unvaped e-liquid (Table 1).^{70–72} Importantly, many other discrete compounds were also detected and determined specifically within the “mint/menthol” flavored e-liquids. These compounds may serve as important biomarkers of harm.

Much is known regarding tobacco smoking as a major risk factor for the development of lung disease and susceptibility to pulmonary disease. However, when vaping, the user inhales a large array of chemicals, including additives, flavors, and nicotine, which are potentially highly toxic, e.g., formaldehyde and acrolein, a chemical often found in weed killers. After the vaping process, chemical reactions of these constituents can generate even more harmful chemicals in the produced aerosol and vapor, which differ between flavored versus tobacco or unflavored e-liquid products. This study and our other reports (as well as work performed by other groups) suggest cytotoxicity and inflammatory effects associated with e-liquid

usage.^{65,73–76} Within the cigarette smoke-exposed lung, alveolar macrophages (AM) have demonstrated a phagocytosis defect, which is a key characteristic of the lung's innate immune response.⁷⁷ This characteristic is key to the innate immune response in the lung. Thus, there is the potential that vaping may exert a similar effect.

The overall impact of vaping on human health also likely lies with its impact on these immune cell populations, in particular, the role of vaping in immune dysfunction and inflammation. Tobacco exposure triggers a number of inflammatory responses in the airways, often leading to ailments such as airway inflammation, chronic obstructive pulmonary disease, and lung cancer.⁷⁸ E-cig use is also linked with immunosuppression in the lower airways of vapers.^{79,80} Inhaled e-liquid aerosols are believed to be deposited in these airway areas, that is, in the broncho-alveolar region.⁸¹ Thus, neutrophils and AM, which are two of the major inflammatory cell types involved in lung defense⁸² and situated within this lower airway region, are likely affected.⁸³ A first example with regards to vaping involves human AMs exposed to an e-liquid vapor distillate revealed, with increased levels of ROS production, significantly inhibited phagocytosis and increased levels of several cytokines, e.g., IL-6 and TNF- α , ultimately observed.⁶¹ Similarly, our zebrafish model can assess oxidative stress while our mouse model can be used to investigate pro-inflammatory responses, including pro-inflammatory cytokine levels; a second reported example is more specific with the popular e-liquid flavor chemical cinnamaldehyde possessing dose-dependent broadly immunosuppressive effects: diminished phagocytic capacity (neutrophils and macrophages), pro-inflammatory cytokine production and a cell-mediated cytotoxic response (NK cells).⁸⁴ Thus, we have also further investigated and confirmed that vaping imparts a similar inflammatory profile through the use of our two in vivo models.

■ ASSOCIATED CONTENT

SI Supporting Information

The Supporting Information is available free of charge at <https://pubs.acs.org/doi/10.1021/acsomega.4c03416>.

All identified spectral library matches and NIST-only spectral library matches (XLSX)

■ AUTHOR INFORMATION

Corresponding Author

Vijay Sivaraman – Department of Biological & Biomedical Sciences, North Carolina Central University, Durham, North Carolina 27707, United States; Phone: (919) 530-5564; Email: vijay.sivaraman@ncsu.edu

Authors

Imari Walker-Franklin – RTI International, Research Triangle Park, North Carolina 27704, United States

Rob U. Onyenwoke – Department of Biological & Biomedical Sciences, North Carolina Central University, Durham, North Carolina 27707, United States; Biomanufacturing Research Institute and Technology Enterprise (BRITE), North Carolina Central University, Durham, North Carolina 27707, United States; orcid.org/0000-0002-8568-1575

TinChung Leung – Department of Biological & Biomedical Sciences, North Carolina Central University, Durham, North Carolina 27707, United States; The Julius L. Chambers Biomedical/Biotechnology Research Institute, North Carolina

Central University, North Carolina Research Campus,
Kannapolis, North Carolina 28081, United States

Xiaoyan Huang – The Julius L. Chambers Biomedical/
Biotechnology Research Institute, North Carolina Central
University, North Carolina Research Campus, Kannapolis,
North Carolina 28081, United States

Jeffrey G. Shipman – Department of Biological & Biomedical
Sciences, North Carolina Central University, Durham, North
Carolina 27707, United States

Alex Kovach – RTI International, Research Triangle Park,
North Carolina 27704, United States

Complete contact information is available at:

<https://pubs.acs.org/10.1021/acsomega.4c03416>

Author Contributions

¹I.W.-F. and R.U.O. contributed equally to this work.

Notes

The authors declare no competing financial interest.

ACKNOWLEDGMENTS

This work was supported in part by grants from RCMU-U54 RCHDR (1U54MD012392) from the National Institute of Minority Health Disparities (NIMHD) and the Center for Human Health and the Environment (CHHE, P30ES025128) from the National Institute of Environmental Health Sciences (NIEHS). The content is solely the responsibility of the authors and does not necessarily represent the official views of the National Institutes of Health. The Table of Contents Graphic was created with [BioRender.com](https://www.biorender.com).

ADDITIONAL NOTE

^aAmerican Lung Association (lung.org/quit-smoking/smoking-facts/whats-in-a-cigarette).

REFERENCES

- (1) Behar, R. Z.; Wang, Y.; Talbot, P. Comparing the cytotoxicity of electronic cigarette fluids, aerosols and solvents. *Tobac. Control* **2018**, *27*, 325–333.
- (2) Omaiye, E. E.; McWhirter, K. J.; Luo, W.; Pankow, J. F.; Talbot, P. High-Nicotine Electronic Cigarette Products: Toxicity of JUUL Fluids and Aerosols Correlates Strongly with Nicotine and Some Flavor Chemical Concentrations. *Chem. Res. Toxicol.* **2019**, *32*, 1058–1069.
- (3) Singh, J.; Luquet, E.; Smith, D. P. T.; Potgieter, H. J.; Ragazzon, P. Toxicological and analytical assessment of e-cigarette refill components on airway epithelia. *Sci. Prog.* **2016**, *99*, 351–398.
- (4) Pinkston, R.; Zaman, H.; Hossain, E.; Penn, A. L.; Noel, A. Cell-specific toxicity of short-term JUUL aerosol exposure to human bronchial epithelial cells and murine macrophages exposed at the air-liquid interface. *Respir. Res.* **2020**, *21*, 269.
- (5) Pinkston, R.; Penn, A. L.; Noel, A. Increased oxidative stress responses in murine macrophages exposed at the air-liquid interface to third- and fourth-generation electronic nicotine delivery system (ENDS) aerosols. *Toxicol. Rep.* **2023**, *11*, 40–57.
- (6) Arrazola, R. A.; Kuiper, N. M.; Dube, S. R. Patterns of current use of tobacco products among U.S. high school students for 2000–2012—findings from the National Youth Tobacco Survey. *J. Adolesc. Health* **2014**, *54*, 54.
- (7) Arrazola, R. A.; Ahluwalia, I. B.; Pun, E.; Garcia de Quevedo, I.; Babb, S.; Armour, B. S. Current Tobacco Smoking and Desire to Quit Smoking Among Students Aged 13–15 Years - Global Youth Tobacco Survey, 61 Countries, 2012–2015. *MMWR Morb. Mortal. Wkly. Rep.* **2017**, *66*, 533–537.
- (8) Besaratinia, A.; Tommasi, S. An opportune and unique research to evaluate the public health impact of electronic cigarettes. *Cancer Causes Control* **2017**, *28*, 1167–1171.
- (9) Ali, F. R. M.; Seidenberg, A. B.; Crane, E.; Seaman, E.; Tynan, M. A.; Marynak, K. E-cigarette Unit Sales by Product and Flavor Type, and Top-Selling Brands, United States, 2020–2022. *MMWR Morb. Mortal. Wkly. Rep.* **2023**, *72*, 672–677.
- (10) Ali, F. R. M.; Seaman, E. L.; Crane, E.; Schillo, B.; King, B. A. Trends in US E-cigarette Sales and Prices by Nicotine Strength, Overall and by Product and Flavor Type, 2017–2022. *Nicotine Tob. Res.* **2023**, *25*, 1052–1056.
- (11) Sassano, M. F.; Ghosh, A.; Tarran, R. Tobacco Smoke Constituents Trigger Cytoplasmic Calcium Release. *Appl. In Vitro Toxicol.* **2017**, *3*, 193–198.
- (12) Davis, E. S.; Sassano, M. F.; Goodell, H.; Tarran, R. E-Liquid Autofluorescence can be used as a Marker of Vaping Deposition and Third-Hand Vape Exposure. *Sci. Rep.* **2017**, *7*, 7459.
- (13) Sassano, M. F.; Davis, E. S.; Keating, J. E.; Zorn, B. T.; Kochar, T. K.; Wolfgang, M. C.; Glish, G. L.; Tarran, R. Evaluation of e-liquid toxicity using an open-source high-throughput screening assay. *PLoS Biol.* **2018**, *16*, No. e2003904.
- (14) Etter, J. F.; Bullen, C. Saliva cotinine levels in users of electronic cigarettes. *Eur. Respir. J.* **2011**, *38*, 1219–1220.
- (15) Riker, C. A.; Lee, K.; Darville, A.; Hahn, E. J. E-cigarettes: promise or peril? *Nurs. Clin. North Am.* **2012**, *47*, 159–171.
- (16) Wall, M. A.; Johnson, J.; Jacob, P.; Benowitz, N. L. Cotinine in the serum, saliva, and urine of nonsmokers, passive smokers, and active smokers. *Am. J. Pub. Health* **1988**, *78*, 699–701.
- (17) Zhu, S.-H.; Sun, J. Y.; Bonnevie, E.; Cummins, S. E.; Gamst, A.; Yin, L.; Lee, M. Four hundred and sixty brands of e-cigarettes and counting: implications for product regulation. *Tobac. Control* **2014**, *23*, iii3–iii9.
- (18) Besaratinia, A.; Tommasi, S. Electronic cigarettes: the road ahead. *Prev. Med.* **2014**, *66*, 65–67.
- (19) Goniewicz, M. L.; Knysak, J.; Gawron, M.; Kosmider, L.; Sobczak, A.; Kurek, J.; Prokopowicz, A.; Jablonska-Czapla, M.; Rosik-Dulewska, C.; Havel, C.; et al. Levels of selected carcinogens and toxicants in vapour from electronic cigarettes. *Tobac. Control* **2014**, *23*, 133–139.
- (20) Hua, M.; Omaiye, E. E.; Luo, W.; McWhirter, K. J.; Pankow, J. F.; Talbot, P. Identification of Cytotoxic Flavor Chemicals in Top-Selling Electronic Cigarette Refill Fluids. *Sci. Rep.* **2019**, *9*, 2782.
- (21) Williams, M.; Villarreal, A.; Bozhilov, K.; Lin, S.; Talbot, P. Metal and silicate particles including nanoparticles are present in electronic cigarette cartomizer fluid and aerosol. *PloS One* **2013**, *8*, No. e57987.
- (22) Allen, J. G.; Flanigan, S. S.; LeBlanc, M.; Vallarino, J.; MacNaughton, P.; Stewart, J. H.; Christiani, D. C. Flavoring Chemicals in E-Cigarettes: Diacetyl, 2,3-Pentanedione, and Acetoin in a Sample of 51 Products, Including Fruit-Candy-and Cocktail-Flavored E-Cigarettes. *Environ. Health Perspect.* **2016**, *124*, 733–739.
- (23) Barker, A. F.; Bergeron, A.; Rom, W. N.; Hertz, M. I. Obliterative bronchiolitis. *N. Engl. J. Med.* **2014**, *370*, 1820–1828.
- (24) Kreiss, K.; Gomaa, A.; Kullman, G.; Fedan, K.; Simoes, E. J.; Enright, P. L. Clinical bronchiolitis obliterans in workers at a microwave-popcorn plant. *N. Engl. J. Med.* **2002**, *347*, 330–338.
- (25) Leventhal, A. M.; Tackett, A. P.; Whitted, L.; Jordt, S. E.; Jabba, S. V. Ice flavours and non-menthol synthetic cooling agents in e-cigarette products: a review. *Tobac. Control* **2023**, *32*, 769–777.
- (26) Pankow, J. F.; Luo, W.; McWhirter, K. J.; Gillette, S.; Cohen, J. E. 'Menthol-Plus': a major category of cigarette found among 'concept' descriptor cigarettes from Mexico. *Tobac. Control* **2022**, *31*, e18–e24.
- (27) Leventhal, A.; Dai, H.; Barrington-Trimis, J.; Sussman, S. 'Ice' flavoured e-cigarette use among young adults. *Tobac. Control* **2023**, *32*, 114–117.
- (28) Behar, R. Z.; Luo, W.; McWhirter, K. J.; Pankow, J. F.; Talbot, P. Analytical and toxicological evaluation of flavor chemicals in electronic cigarette refill fluids. *Sci. Rep.* **2018**, *8*, 8288.

- (29) Bahl, V.; Lin, S.; Xu, N.; Davis, B.; Wang, Y. h.; Talbot, P. Comparison of electronic cigarette refill fluid cytotoxicity using embryonic and adult models. *Reprod. Toxicol.* **2012**, *34*, 529–537.
- (30) Krusemann, E. J. Z.; Boesveldt, S.; de Graaf, K.; Talhout, R. An E-Liquid Flavor Wheel: A Shared Vocabulary Based on Systematically Reviewing E-Liquid Flavor Classifications in Literature. *Nicotine Tob. Res.* **2019**, *21*, 1310–1319.
- (31) Kavuluru, R.; Han, S.; Hahn, E. J. On the popularity of the USB flash drive-shaped electronic cigarette Juul. *Tobac. Control* **2018**, *28*, 110.
- (32) Dai, H.; Hao, J. Online popularity of JUUL and Puff Bars in the USA: 2019–2020. *Tobac. Control* **2022**, *31*, 7–10.
- (33) Zhang, R.; Jones, M. M.; Dornsife, R. E.; Wu, T.; Sivaraman, V.; Tarran, R.; Onyenwoke, R. U. JUUL e-liquid exposure elicits cytoplasmic Ca(2+) responses and leads to cytotoxicity in cultured airway epithelial cells. *Toxicol. Lett.* **2021**, *337*, 46–56.
- (34) Ghosh, A.; Beyazcicek, O.; Davis, E. S.; Onyenwoke, R. U.; Tarran, R. Cellular effects of nicotine salt-containing e-liquids. *J. Appl. Toxicol.* **2021**, *41*, 493–505.
- (35) Onyenwoke, R. U.; Leung, T.; Huang, X.; Parker, D.; Shipman, J. G.; Alhadyan, S. K.; Sivaraman, V. An assessment of vaping-induced inflammation and toxicity: A feasibility study using a 2-stage zebrafish and mouse platform. *Food Chem. Toxicol.* **2022**, *163*, 112923.
- (36) Panitz, D.; Swamy, H.; Nehrke, K. A. C. A C. elegans model of electronic cigarette use: Physiological effects of e-liquids in nematodes. *BMC Pharmacol. Toxicol.* **2015**, *16*, 32.
- (37) Sivaraman, V.; Parker, D.; Zhang, R.; Jones, M. M.; Onyenwoke, R. U. Vaping Exacerbates Coronavirus-Related Pulmonary Infection in a Murine Model. *Front. Physiol.* **2021**, *12*, 634839.
- (38) Koelmel, J. P.; Xie, H.; Price, E. J.; Lin, E. Z.; Manz, K. E.; Stelben, P.; Paige, M. K.; Papazian, S.; Okeme, J.; Jones, D. P.; et al. An actionable annotation scoring framework for gas chromatography-high-resolution mass spectrometry. *Exposome* **2022**, *2*, osac007.
- (39) Cassar, S.; Adatto, I.; Freeman, J. L.; Gamse, J. T.; Iturria, I.; Lawrence, C.; Muriana, A.; Peterson, R. T.; Van Cruchten, S.; Zon, L. I. Use of Zebrafish in Drug Discovery Toxicology. *Chem. Res. Toxicol.* **2020**, *33*, 95–118.
- (40) Shen, W.; Lou, B.; Xu, C.; Yang, G.; Yu, R.; Wang, X.; Li, X.; Wang, Q.; Wang, Y. Lethal toxicity and gene expression changes in embryonic zebrafish upon exposure to individual and mixture of malathion, chlorpyrifos and lambda-cyhalothrin. *Chemosphere* **2020**, *239*, 124802.
- (41) Elerse, T.; Novak, M.; Mlinar, M.; Virant, I.; Babor, N.; Leben, K.; Žegura, B.; Filipič, M. Lethal and Sub-Lethal Effects and Modulation of Gene Expression Induced by T Kinase Inhibitors in Zebrafish (*Danio Rerio*) Embryos. *Toxics* **2021**, *10*, 4.
- (42) Ducharme, N. A.; Peterson, L. E.; Benfenati, E.; Reif, D.; McCollum, C. W.; Gustafsson, J. Å.; Bondesson, M. Meta-analysis of toxicity and teratogenicity of 133 chemicals from zebrafish developmental toxicity studies. *Reprod. Toxicol.* **2013**, *41*, 98–108.
- (43) Tsujita, T.; Li, L.; Nakajima, H.; Iwamoto, N.; Nakajima-Takagi, Y.; Ohashi, K.; Kawakami, K.; Kumagai, Y.; Freeman, B. A.; Yamamoto, M.; et al. Nitro-fatty acids and cyclopentenone prostaglandins share strategies to activate the Keap1-Nrf2 system: a study using green fluorescent protein transgenic zebrafish. *Genes Cells* **2011**, *16*, 46–57.
- (44) Finlay, B. L.; Darlington, R. B. Linked regularities in the development and evolution of mammalian brains. *Science* **1995**, *268*, 1578–1584.
- (45) Spindle, T. R.; Talih, S.; Hiler, M. M.; Karaoglanian, N.; Halquist, M. S.; Breland, A. B.; Shihadeh, A.; Eissenberg, T. Effects of electronic cigarette liquid solvents propylene glycol and vegetable glycerin on user nicotine delivery, heart rate, subjective effects, and puff topography. *Drug Alcohol Depend.* **2018**, *188*, 193–199.
- (46) Lee, J. H.; Hailey, K. L.; Vitorino, S. A.; Jennings, P. A.; Bigby, T. D.; Breen, E. C. Cigarette Smoke Triggers IL-33-associated Inflammation in a Model of Late-Stage Chronic Obstructive Pulmonary Disease. *Am. J. Respir. Cell Mol. Biol.* **2019**, *61*, 567–574.
- (47) Crotty Alexander, L. E.; Drummond, C. A.; Hepokoski, M.; Mathew, D.; Moshensky, A.; Willeford, A.; Das, S.; Singh, P.; Yong, Z.; Lee, J. H.; et al. Chronic inhalation of e-cigarette vapor containing nicotine disrupts airway barrier function and induces systemic inflammation and multiorgan fibrosis in mice. *Am. J. Physiol.: Regul., Integr. Comp. Physiol.* **2018**, *314*, R834–R847.
- (48) Maikawa, C. L.; Zimmerman, N.; Ramos, M.; Shah, M.; Wallace, J.; Pollitt, K. Comparison of Airway Responses Induced in a Mouse Model by the Gas and Particulate Fractions of Gasoline Direct Injection Engine Exhaust. *Int. J. Environ. Res. Public Health* **2018**, *15*, 429.
- (49) Harris, B.; McAlister, A.; Willoughby, T.; Sivaraman, V. Alcohol-dependent pulmonary inflammation: A role for HMGB-1. *Alcohol* **2019**, *80*, 45–52.
- (50) Zhang, R.; Jones, M. M.; Parker, D.; Dornsife, R. E.; Wymer, N.; Onyenwoke, R. U.; Sivaraman, V. Acute vaping exacerbates microbial pneumonia due to calcium (Ca2+) dysregulation. *PLoS One* **2021**, *16*, No. e0256166.
- (51) Willingham, S. B.; Allen, I. C.; Bergstralh, D. T.; Brickey, W. J.; Huang, M. T. H.; Taxman, D. J.; Duncan, J. A.; Ting, J. P. Y. NLRP3 (NALP3, Cryopyrin) facilitates in vivo caspase-1 activation, necrosis, and HMGB1 release via inflammasome-dependent and -independent pathways. *J. Immunol.* **2009**, *183*, 2008–2015.
- (52) Kristiansen, U.; Vinggaard, A. M.; Nielsen, G. D. The effects of n-butanol vapour on respiratory rate and tidal volume. *Arch. Toxicol.* **1988**, *61*, 229–236.
- (53) Ford, R. A.; Api, A. M.; Suskind, R. R. Allergic contact sensitization potential of hydroxycitronellal in humans. *Food Chem. Toxicol.* **1988**, *26*, 921–926.
- (54) d'Alencón, C. A.; Peña, O. A.; Wittmann, C.; Gallardo, V. E.; Jones, R. A.; Loosli, F.; Liebel, U.; Grabher, C.; Allende, M. L. A high-throughput chemically induced inflammation assay in zebrafish. *BMC Biol.* **2010**, *8*, 151.
- (55) Ngo, V.; Duennwald, M. L. Nrf2 and Oxidative Stress: A General Overview of Mechanisms and Implications in Human Disease. *Antioxidants* **2022**, *11*, 2345.
- (56) Ma, Q. Role of nrf2 in oxidative stress and toxicity. *Annu. Rev. Pharmacol. Toxicol.* **2013**, *53*, 401–426.
- (57) Zhu, Y.; Wang, P.; Zhao, Y.; Yang, C.; Clark, A.; Leung, T.; Chen, X.; Sang, S. Synthesis, evaluation, and metabolism of novel [6]-shogaol derivatives as potent Nrf2 activators. *Free Radicals Biol. Med.* **2016**, *95*, 243–254.
- (58) Parker, J. C.; Townsley, M. I. Evaluation of lung injury in rats and mice. *Am. J. Physiol. Lung Cell. Mol. Physiol.* **2004**, *286*, L231–L246.
- (59) Xu, T.; Qiao, J.; Zhao, L.; Wang, G.; He, G.; Li, K.; Tian, Y.; Gao, M.; Wang, J.; Wang, H.; et al. Acute respiratory distress syndrome induced by avian influenza A (H5N1) virus in mice. *Am. J. Respir. Crit. Care Med.* **2006**, *174*, 1011–1017.
- (60) Lerner, C. A.; Sundar, I. K.; Yao, H.; Gerloff, J.; Ossip, D. J.; McIntosh, S.; Robinson, R.; Rahman, I. Vapors produced by electronic cigarettes and e-juices with flavorings induce toxicity, oxidative stress, and inflammatory response in lung epithelial cells and in mouse lung. *PLoS One* **2015**, *10*, No. e0116732.
- (61) Scott, A.; Lugg, S. T.; Aldridge, K.; Lewis, K. E.; Bowden, A.; Mahida, R. Y.; Grudzinska, F. S.; Dosanjh, D.; Parekh, D.; Foronjy, R.; et al. Pro-inflammatory effects of e-cigarette vapour condensate on human alveolar macrophages. *Thorax* **2018**, *73*, 1161–1169.
- (62) Misra, M.; Leverette, R. D.; Cooper, B. T.; Bennett, M. B.; Brown, S. E. Comparative in vitro toxicity profile of electronic and tobacco cigarettes, smokeless tobacco and nicotine replacement therapy products: e-liquids, extracts and collected aerosols. *Int. J. Environ. Res. Public Health* **2014**, *11*, 11325–11347.
- (63) Zahedi, A.; Phandthong, R.; Chaili, A.; Leung, S.; Omaiye, E.; Talbot, P. Mitochondrial Stress Response in Neural Stem Cells Exposed to Electronic Cigarettes. *iScience* **2019**, *16*, 250–269.
- (64) Rowell, T. R.; Reeber, S. L.; Lee, S. L.; Harris, R. A.; Nethery, R. C.; Herring, A. H.; Glish, G. L.; Tarran, R. Flavored E-cigarette Liquids Reduce Proliferation and Viability in the CALU3 Airway

Epithelial Cell Line. *Am. J. Physiol. Lung Cell. Mol. Physiol.* **2017**, *313*, L52–L66.

(65) Rowell, T. R.; Tarran, R. Will chronic e-cigarette use cause lung disease? *Am. J. Physiol. Lung Cell. Mol. Physiol.* **2015**, *309*, L1398–L1409.

(66) Chen, W.; Wang, P.; Ito, K.; Fowles, J.; Shusterman, D.; Jaques, P. A.; Kumagai, K. Measurement of heating coil temperature for e-cigarettes with a "top-coil" clearomizer. *PLoS One* **2018**, *13*, No. e0195925.

(67) Doolittle, D. J.; Lee, C. K.; Ivett, J. L.; Mirsalis, J. C.; Riccio, E.; Rudd, C. J.; Burger, G. T.; Hayes, A. W. Comparative studies on the genotoxic activity of mainstream smoke condensate from cigarettes which burn or only heat tobacco. *Environ. Mol. Mutagen.* **1990**, *15*, 93–105.

(68) Khlystov, A.; Samburova, V. Flavoring Compounds Dominate Toxic Aldehyde Production during E-Cigarette Vaping. *Environ. Sci. Technol.* **2016**, *50*, 13080–13085.

(69) Guo, W.; Vrdoljak, G.; Liao, V. C.; Moezzi, B. Major Constituents of Cannabis Vape Oil Liquid, Vapor and Aerosol in California Vape Oil Cartridge Samples. *Front. Chem.* **2021**, *9*, 694905.

(70) Muthumalage, T.; Friedman, M. R.; McGraw, M. D.; Ginsberg, G.; Friedman, A. E.; Rahman, I. Chemical Constituents Involved in E-Cigarette, or Vaping Product Use-Associated Lung Injury (EVALI). *Toxics* **2020**, *8*, 25.

(71) Lu, S. J.; Li, L.; Duffy, B. C.; Dittmar, M. A.; Durocher, L. A.; Panawennage, D.; Delaney-Baldwin, E. R.; Spink, D. C. Investigation of Vaping Fluids Recovered From New York State E-Cigarette or Vaping Product Use-Associated Lung Injury Patients. *Front. Chem.* **2021**, *9*, 748935.

(72) Jiang, H.; Ahmed, C. M. S.; Martin, T. J.; Canchola, A.; Oswald, I. W. H.; Garcia, J. A.; Chen, J. Y.; Koby, K. A.; Buchanan, A. J.; Zhao, Z.; et al. Chemical and Toxicological Characterization of Vaping Emission Products from Commonly Used Vape Juice Diluents. *Chem. Res. Toxicol.* **2020**, *33*, 2157–2163.

(73) Ghosh, A.; Coakley, R. C.; Mascenik, T.; Rowell, T. R.; Davis, E. S.; Rogers, K.; Webster, M. J.; Dang, H.; Herring, L. E.; Sassano, M. F.; et al. Chronic E-Cigarette Exposure Alters the Human Bronchial Epithelial Proteome. *Am. J. Respir. Crit. Care Med.* **2018**, *198*, 67–76.

(74) Vlahos, R. E-Cigarettes: Inducing Inflammation that Spans Generations. *Am. J. Respir. Cell Mol. Biol.* **2018**, *58*, 286–287.

(75) Shields, P. G.; Berman, M.; Brasky, T. M.; Freudenheim, J. L.; Mathe, E.; McElroy, J. P.; Song, M. A.; Wewers, M. D. A Review of Pulmonary Toxicity of Electronic Cigarettes in the Context of Smoking: A Focus on Inflammation. *Cancer Epidemiol. Biomarkers Prev.* **2017**, *26*, 1175–1191.

(76) ArRejaie, A. S.; Al-Aali, K. A.; Alrabiah, M.; Vohra, F.; Mokeem, S. A.; Basunbul, G.; Alrahlah, A.; Abduljabbar, T. Proinflammatory cytokine levels and peri-implant parameters among cigarette smokers, individuals vaping electronic cigarettes and non-smokers. *J. Periodontol.* **2019**, *90*, 367–374.

(77) Karavitis, J.; Kovacs, E. J. Macrophage phagocytosis: effects of environmental pollutants, alcohol, cigarette smoke, and other external factors. *J. Leukoc. Biol.* **2011**, *90*, 1065–1078.

(78) Rom, O.; Avezov, K.; Aizenbud, D.; Reznick, A. Z. Cigarette smoking and inflammation revisited. *Respir. Physiol. Neurobiol.* **2013**, *187*, 5–10.

(79) Martin, E. M.; Clapp, P. W.; Rebuli, M. E.; Pawlak, E. A.; Glista-Baker, E.; Benowitz, N. L.; Fry, R. C.; Jaspers, I. E-cigarette use results in suppression of immune and inflammatory-response genes in nasal epithelial cells similar to cigarette smoke. *Am. J. Physiol. Lung Cell. Mol. Physiol.* **2016**, *311*, L135–L144.

(80) Reidel, B.; Radicioni, G.; Clapp, P. W.; Ford, A. A.; Abdelwahab, S.; Rebuli, M. E.; Haridass, P.; Alexis, N. E.; Jaspers, I.; Kesimer, M. E-Cigarette Use Causes a Unique Innate Immune Response in the Lung, Involving Increased Neutrophilic Activation and Altered Mucin Secretion. *Am. J. Respir. Crit. Care Med.* **2018**, *197*, 492–501.

(81) Zhang, Y.; Sumner, W.; Chen, D. R. In vitro particle size distributions in electronic and conventional cigarette aerosols suggest

comparable deposition patterns. *Nicotine Tob. Res.* **2013**, *15*, 501–508.

(82) Sibille, Y.; Reynolds, H. Y. Macrophages and polymorphonuclear neutrophils in lung defense and injury. *Am. Rev. Respir. Dis.* **1990**, *141*, 471–501.

(83) Ghosh, A.; Coakley, R. D.; Ghio, A. J.; Muhlebach, M. S.; Esther, C. R.; Alexis, N. E.; Tarran, R. Chronic E-Cigarette Use Increases Neutrophil Elastase and Matrix Metalloprotease Levels in the Lung. *Am. J. Respir. Crit. Care Med.* **2019**, *200*, 1392–1401.

(84) Clapp, P. W.; Pawlak, E. A.; Lackey, J. T.; Keating, J. E.; Reeber, S. L.; Glish, G. L.; Jaspers, I. Flavored e-cigarette liquids and cinnamaldehyde impair respiratory innate immune cell function. *Am. J. Physiol. Lung Cell. Mol. Physiol.* **2017**, *313*, L278–L292.